ROS-Based 3D On-Line Monitoring of LMD Robotized Cells

Jorge Rodríguez-Araújo[1], Juan J. Rodríguez-Andina[2]
[1]AIMEN Technology Center, Porriño, Spain
[2]Department of Electronic Technology, University of Vigo, Vigo, Spain
jorge.rodriguez@aimen.es, jjrdguez@uvigo.es

***Abstract*— Laser Metal Deposition (LMD) is a promising technique for fabrication of large metallic parts directly from 3D CAD models. However, the complexity of the process makes it challenging to prevent geometrical distortions and defects to affect the fabricated parts. On-line monitoring and control are fundamental issues to mitigate these problems, but they are not efficiently enough provided by current LMD techniques. As the first step in the development of an efficient unified on-line monitoring and control system for LMD, this paper presents a novel on-line 3D monitoring system for part geometry measurement. The system is capable of working in real-time in robot coordinates, without imposing restrictions to the possible paths, orientations or speed of movement. The use of ROS and the self-calibration method also proposed in the paper provide a flexible, cost-effective solution to easily upgrade current industrial LMD robotized cells. Experimental results support the practical feasibility of the proposed solution.**

I. INTRODUCTION

Laser Metal Deposition (LMD) is a promising additive-manufacturing technique for repair or fabrication of near-net-shape (i.e., close to the target final shape) metallic parts. These are built up layer by layer directly from a 3D CAD model, through the successive deposition of (partially) overlapped clad tracks using laser cladding [1]. In laser cladding, a laser beam is used to melt metallic powder particles injected on the surface of the target part while the cladding system moves along a predefined path. This process is very popular in industry for coating and repair of critical parts, such as turbine blades or stamping molds.

It has been traditionally assumed that no distortions affect the laser cladding process, and hence a set of fixed, predefined process parameters (e.g., speed, laser power, powder feed rate) can be used through the successive deposition of layers. Therefore, the laser tracks required to build up a given part are determined off-line, based on the assumption of constant layer height and width.

In practice, however, the complexity of laser cladding makes it challenging to obtain homogeneous layers with specific metallurgical or mechanical properties, because the characteristics of the deposited layers are affected by heating (this fact is more significant in large parts) and they also depend on the target geometry. As a consequence, fabricated parts may suffer from clad defects and geometric distortions. Overheating and accumulation of residual thermal stresses are the main causes of fabrication defects. To prevent all these problems, suitable LMD monitoring and control systems are required.

In recent years, several closed-loop control systems have been proposed to improve the performance of laser cladding processes [2]-[4]. These systems use a coaxial arrangement for monitoring melt pool temperature or width, and act on laser power to compensate the effects of thermal variations. A more complex solution, based on an off-axis setup with three CCD cameras, is proposed in [5] to improve the dimensional accuracy of a direct metal deposition process by controlling melt pool height. However, simpler and more flexible solutions are needed for LMD to better comply with the requirements currently demanded from fabrication processes.

In this context, the ability to perform on-line monitoring is a very important feature not efficiently enough provided by existing LMD dimensional monitoring approaches, like [6], because they cannot work in robot coordinates unless restrictions are imposed to the movements than can be made. Efficient on-line monitoring should allow LMD control parameters to be dynamically adapted to obtain the best possible characteristics and dimensional accuracy in the fabricated parts. In order for this to be possible, two main issues must be addressed, namely:

- To develop an on-line 3D track monitoring system, capable of identifying even small geometric deviations and superficial clad defects.
- To develop an on-line path planner and control system, capable of dynamically adapting process parameters and modifying the trajectories of the robot that performs the movements to create the paths, so as to correct the aforementioned deviations and defects.

A unified monitoring and control solution combining both aspects would be useful not only for fabrication of new parts, but also for automated repair of damaged or aged ones. As a first step in the development of such solution, this paper presents a cost-effective and flexible 3D 6-DoF (Degrees of Freedom) robotized scanning system for on-line LMD monitoring, capable of performing measurements in robot coordinates with no motion constraints in any of the 6

978-1-4799-6649-3/15/$31.00 ©2015 IEEE

degrees of freedom. A novel self-calibration method (directly implemented in the robot) has been developed for the optical system. The capabilities of the proposed approach have been validated in a real industrial LMD cell, demonstrating that on-line measurements can be easily carried out while achieving good enough accuracy. In order for this solution to be easily applied in different existing industrial facilities at a low cost, it has been developed based on open-source Robot Operating System (ROS). In this way, a robot-independent system is obtained.

The remainder of the paper is structured as follows. The proposed solution is first briefly outlined in Section II, and then described in detail in Sections III and IV, where the novel 3D geometrical monitoring and self-calibration systems are respectively introduced. Experimental results are presented and discussed in Section V. Finally, the conclusions of the work are summarized in Section VI.

II. Proposed Solution

A traditional laser cladding cell consists of a solid-state laser fiber coupled with a cladding head, a powder feeder with a coaxial nozzle, and a motion system based on an anthropomorphic industrial robot. The integration through a field bus of this equipment and an off-line programming system completes a typical industrial LMD robotized cell. Its operation can be described from the steps depicted on the left side of Fig. 1:

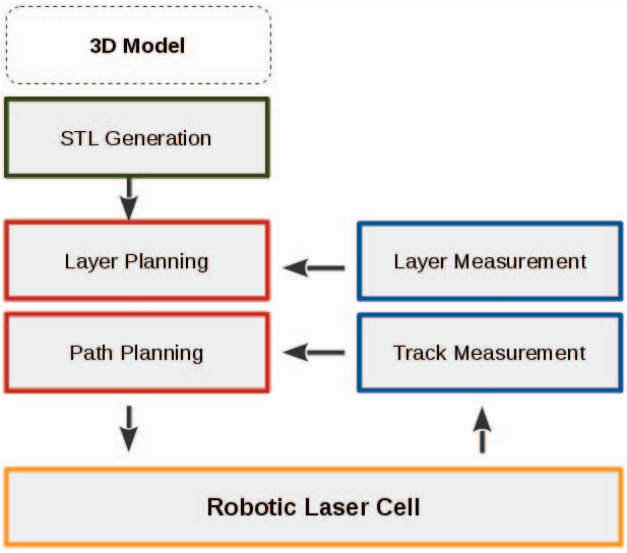

Fig. 1. Industrial LMD robotized cell with on-line monitoring capabilities.

- The target part is described by a 3D CAD model.
- *STL Generation*. The model is analyzed to identify shapes that cannot be fabricated because of mechanical limitations of the cell, resulting in a simplified mesh.
- *Layer Planning*. The volume to be fabricated is divided in slices of equal height from bottom to top.
- *Path Planning*. The paths required to fill each one of the shapes defined in the previous step are identified. From this information the program to be executed by the robot is generated and loaded into it.

The proposed solution is aimed at being compatible with current coaxial systems, providing them with on-line monitoring and control parameter adaptation capabilities, with the advantages described in Section I, both in terms of better performance and flexibility. Therefore, the steps listed above have to be complemented with others in charge of measuring the successive tracks deposited and the resulting layers, and take the control actions required to compensate any geometric deviation or clad defect. As mentioned before, this paper addresses the development of the on-line monitoring system, allowing the two steps on the right of Fig. 1, namely *Track* and *Layer Measurement*, to be added. This will open the door for the implementation of a control system with on-line parameter adaptation capabilities.

Geometric information in 3D is obtained in the form of a cloud of 3D points. Following the usual procedure in many industrial scanner systems, the 3D laser triangulation principle has been applied with this purpose, using an industrial CMOS camera and a laser stripe attached to the laser cladding head (Fig. 2).

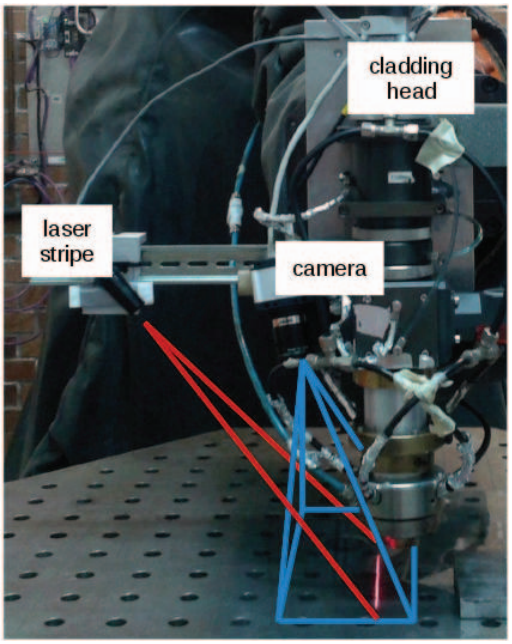

Fig. 2. 3D laser triangulation.

The laser stripe is projected onto the scene, so an illuminated point in the 3D space corresponds to a pixel in the captured image. The coordinates of each illuminated point (3D profile) are computed by triangulation in the camera's coordinate system. The 3D point cloud is then obtained from the instantaneous robot tool pose (position and orientation). In order for good accuracy to be achieved, a precise calibration of the optical system is required. Therefore, two main processes have to be carried out:

- *3D geometrical monitoring*, consisting of laser stripe detection, laser triangulation, and transformation to robot coordinates to obtain the points in the 3D cloud. The implementation of this task in the proposed system is presented in Section III. It has been written in C++ and

integrated using ROS-Industrial, providing an open-source, robot-independent solution.

- *Calibration*, i.e., accurate identification of the geometric parameters of the system required to obtain the 3D point cloud in robot coordinates. A flexible automatic self-calibration procedure, described in Section IV, has been developed with this purpose. It has been written in Python, with OpenCV [7] as main library, again providing an open-source solution.

A more detailed description of the whole process can be made from the block diagram shown in Fig. 3, where the following elements can be identified:

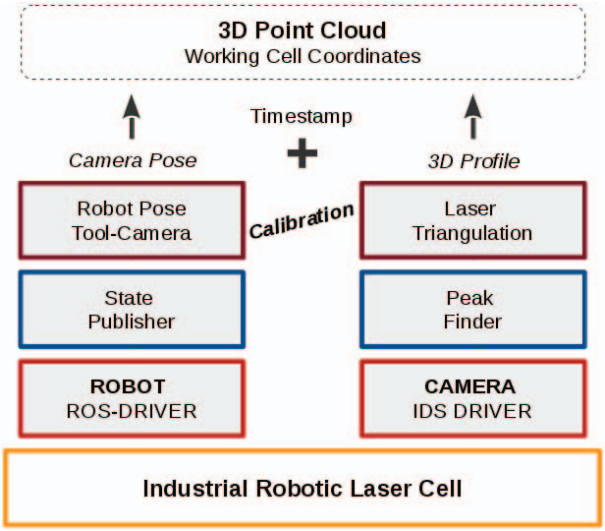

Fig. 3. Proposed solution for on-line 3D point cloud measurement.

- Two *drivers* connected to the LMD robotized cell, one for Ethernet communication with the robot using the ROS-Industrial standard, and another for Gigabit Ethernet image acquisition from the camera.
- *Robot State Publisher*, a standard ROS node allowing instantaneous robot pose to be determined.
- *Peak Finder*, which locates in an image the 2D laser profile, i.e., the points illuminated by the laser stripe.
- *Robot Pose Tool-Camera*, which computes the instantaneous camera pose from the data provided by both the *State Publisher* and the transformation that relates the pose of the camera with that of the robot tool, implemented as part of the *Calibration* process.
- *Laser Triangulation*, which transforms the 2D laser profile (image coordinates) in 3D (real) camera coordinates.
- *Camera Pose + 3D Profile + (timestamp)*, which derives for each time instant (i.e., for each captured image) the 3D point cloud in robot coordinates.

III. 3D Geometrical Monitoring

The purpose of 3D geometrical monitoring is to obtain at each time instant the 3D point cloud (i.e., geometric information about the tracks resulting from the LMD process) in robot coordinates. This has to be accomplished on-line, independently of the speed of movement (within the practical limits of the process) and without the need to apply any restrictions to the possible paths. The three tasks involved in the monitoring process, namely laser stripe detection (*Peak Finder*), laser triangulation, and transformation to robot coordinates to obtain the 3D point cloud, have been implemented in a PC using open-source tools, as stated in Section II. They are described in the following sections.

A. Laser Stripe Detection

The resolution and accuracy of a 3D triangulation system depends on the geometrical arrangement and on the method used to detect the laser stripe. The energy pattern of a laser stripe corresponds to a Gaussian profile. Therefore, a good solution to determine the profile projected by a laser stripe is to identify the pixels in the image that correspond to the maximum (peak) light intensity. This can be accomplished by computing the Center Of Gravity (COG) of each image row as follows:

$$COG = \frac{\sum x_i \cdot P_i}{\sum P_i} \quad (1)$$

In this way, the central point of the stripe in each row is estimated with sub-pixel resolution, by computing the weighted average value of the column (COG) for the pixels (x_i, i being the column) with gray values above a certain threshold, P_i.

B. Laser Triangulation

The triangulation method uses point correspondences to obtain a 2D-to-3D mapping solution. In [8] it is demonstrated that a 4x3 linear transformation matrix can directly convert 2D image coordinates to 3D camera coordinates. A calibration method, like the one proposed in Section IV, is required to estimate the values of the transformation matrix, which encodes both camera intrinsic parameters (excluding distortion coefficients) and laser plane parameters. The 2D-to-3D conversion is shown in Eq. (2) where the COGs (peaks) of all image rows ([u, v]) are mapped to 3D points [X, Y, Z] with a scaling factor s.

$$\begin{bmatrix} s \cdot X \\ s \cdot Y \\ s \cdot Z \\ s \end{bmatrix} = \begin{bmatrix} t_{11} & t_{12} & t_{13} \\ t_{21} & t_{22} & t_{23} \\ t_{31} & t_{32} & t_{33} \\ t_{41} & t_{42} & t_{43} \end{bmatrix} \cdot \begin{bmatrix} u \\ v \\ 1 \end{bmatrix} \quad (2)$$

C. Point Cloud

The 3D point cloud in robot coordinates is derived from the 3D points obtained in camera coordinates. This implies translating the local reference system (camera frame) of each image acquisition step to the working reference system (robot frame). Since the camera is attached to the robot tool, the instantaneous robot tool pose can be used for this purpose, provided the relative transformation from the robot tool frame to the camera frame is known. This information is obtained as part of the calibration process.

Point cloud derivation is based on ROS-Industrial, providing transparent support for different robots. Instant robot pose is published with a frequency of 10 Hz by the robot driver (Fig. 3), and camera pose is determined every time a new image is acquired, using the interpolation methods in the TF ROS library. From this information, the point cloud in robot coordinates is obtained.

IV. Self-Calibration

As justified in Section III, a calibration procedure is necessary to obtain the data required for derivation of the 3D point cloud. A unified self-calibration method has been developed with this purpose. It provides a flexible automatic adjustment to different process requirements, and avoids the need for accurate mechanical positioning parts. In this way, it allows the system to be easily adapted to work with different resolutions and ranges as required for different part sizes.

The proposed procedure uses an inexpensive planar checkerboard pattern and takes advantage from algorithms implemented in open-source OpenCV software. It consists of three main steps, described in the following sections:

1. Camera calibration, where the camera intrinsic parameters and distortion coefficients are determined through a traditional calibration procedure.
2. Laser stripe calibration, where the relative position and orientation of the laser plane with respect to the camera are determined.
3. Hand-eye calibration, where the position and orientation of the camera in the robot configuration are determined.

A calibration script has been implemented in Python, which uses the same set of images for all steps in the process. In addition, it allows camera distortions to be corrected if the camera distortion model is available.

A. Camera Calibration

The pinhole model (the most popular geometric model for a camera) is used for camera calibration with OpenCV. The calibration procedure involves placing a planar checkerboard pattern in front of the sensor with an arbitrary orientation (Fig. 4). The intrinsic camera parameters (i.e., focal length and principal point) and the distortion coefficients can be determined through projective transformation, which minimizes projection errors of the checkerboard corners in the image. Using correspondences between the checkerboard corners and their coordinates in the captured image, the pose of the checkerboard with respect to the camera center can be obtained.

B. Laser Stripe Calibration

The calibration of camera-to-laser coordinate conversion is required for proper operation of the laser triangulation system. This implies obtaining the coefficients of the 4x3 transformation matrix and the scaling coefficient s in Eq. (2). An approach similar to the one described in [9] has been followed, where again only a planar checkerboard placed at arbitrary orientations is required. Interestingly, the proposed method exhibits increased robustness to calibration noise, because outlier points are removed.

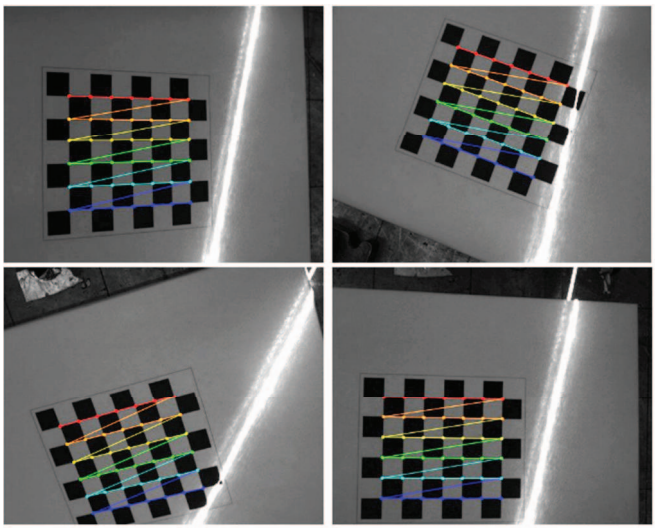

Fig. 4. Automatic checkerboard detection in different perspective positions.

The mapping of 2D image pixels to 3D point coordinates can be determined from a limited set of correspondence points. Since the pose of the checkerboard with respect to the camera center is known, the 3D coordinates of the laser plane intersection with the checkerboard can be determined. This means that the image of the laser stripe can be back-projected onto known world planes. The detected laser stripe is corrected to obtain a best-fit adjustment straight line (Fig. 5), whose points outside the checkerboard are removed. The points in the resulting line are projected from camera to checkerboard coordinates through a planar homographic transformation.

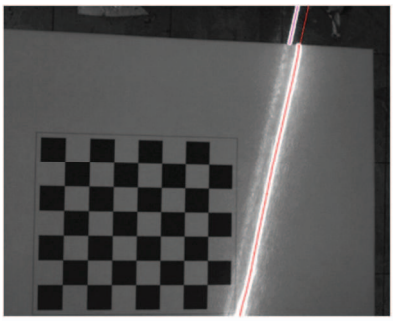

Fig. 5. Sample COG-based (bright pixels) laser stripe detection; red points represent the intersection of the stripe with the target object.

The corners of the checkerboard are used to estimate the homographic transformation matrix with the RANSAC algorithm [10] implemented in OpenCV. The obtained projection matrix and the checkerboard pose are used to transform the laser stripe points to 3D camera coordinates.

A 3D point cloud is derived by processing several calibration pictures. Finding the best-fit plane in this cloud (using an iterative RANSAC method, which minimizes the calculated error), the parameters of the laser plane can be estimated (Eq. (3)). The best-fit plane is defined as the one

that minimizes the orthogonal distance to each point in the 3D point cloud.

$$a \cdot x + b \cdot y + c \cdot z + d = 0 \quad (3)$$

The best-fit laser plane provides correspondences between 3D points and their 2D counterparts in image coordinates through the projective transformation. Hence, to compute the 12 coefficients of the transformation matrix, only 4 non-collinear point correspondences are required. Noise is removed because the 4 points are chosen so as to accurately know their positions in the laser plane.

C. Hand-Eye Calibration

This operation ensures a proper coupling of the camera triangulation system with robot coordinates, without requiring complex camera couplers. The position and orientation of the camera with respect to the robot tool frame is estimated. The camera-to-robot location is calculated using a classical hand-eye method [11] in an automated way.

The calibration of robot-mounted camera is made by solving homogeneous transform equations of the form A·X = X·B, where A is the change in robot tool pose, B is the resulting camera displacement, and X is the camera pose relative to the robot tool. The camera mounting position is determined by moving the robot and observing the resulting image movement. Finally, the checkerboard pose is obtained for each calibration picture, and the corresponding robot tool pose is associated to it.

V. Experimental Results

A. Experimental Setup

The proposed system has been integrated in a typical industrial laser cladding cell, as shown in Fig. 6, where the camera perspective and the laser stripe projection on the working table can be observed. The cell uses a 3.3kW LaserLine LDL 160-3300 diode laser (adjusted to generate the slimmest possible beam), mounted on a 6-axis IRB 4400 robot system from ABB. A Medicoat feeder generates a flow of powder material that concentrates (using a coaxial nozzle) on the target substrate area together with the laser beam focus. The 6-axis robot is used to move the laser beam along the target paths. All process parameters (e.g., laser power, powder feed rate) are controlled from the robot via Profibus.

An IDS µEye industrial camera with a 1.3Mpixel CMOS NIR sensor is used to capture images of the laser stripe line with low noise, at 25fps. It has an optical objective with 12mm focal length providing a field-of-view of about 130x110mm^2 when placed at 250mm of the working table. These conditions have been chosen as a tradeoff between resolution and scanning area. Images are transferred to the monitoring PC using the GigE Vision interface. A chromatic filter adapted to the spectral range of the laser beam is used to improve laser stripe detection.

Monitoring tasks have been implemented in a PC with an Intel i5 Dual Core processor working at 3GHz and 4GB of RAM, running ROS Indigo under Ubuntu 14.04. As stated in Section II, the corresponding code has been written in Python and C++ aiming at real-time execution.

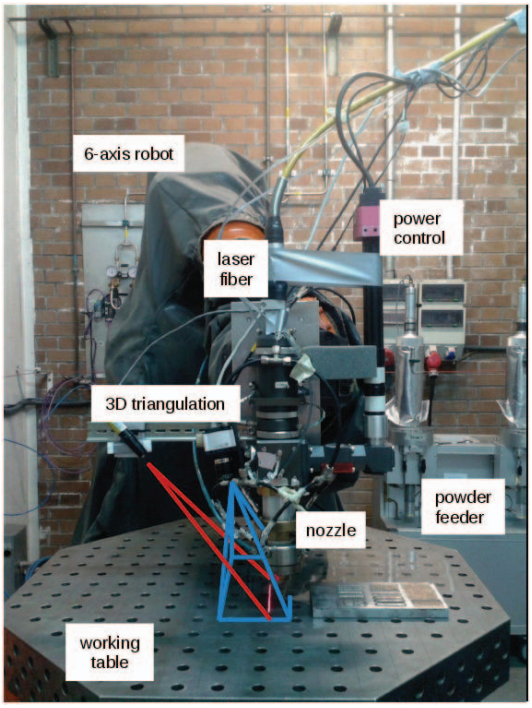

Fig. 6. Setup of the industrial laser cladding cell used in the experiments.

B. System Calibration

The system is calibrated by executing a routine that captures images of an 8x7 pattern of black and white 10mm-side squares (see Figs. 4 and 5) placed on the target viewing area. The quality of this checkerboard does not need to be particularly high. The one used in this work was just laser printed in a piece of regular paper. The checkerboard must cover most of (but not necessarily all) the field-of-view of the camera.

After placing the checkerboard on the working table and the camera over it, the robot is moved to capture images of several different areas of the checkerboard, taking into consideration that the hand-eye calibration algorithm requires large orientation changes between consecutive images to work. Immediately after each robot move, an image is captured. In order for the procedure to run in an automatic way, it is necessary that the laser line moves over the outer part (outer squares) of the checkerboard, and not over the inner one.

Hand-eye calibration is accomplished by using the computed checkerboard poses and the associated robot tool poses (provided by the ROS driver). This allows any point in pixel coordinates to be converted into a 3D point in actual robot coordinates.

C. Processing Results

The proposed system has just being installed in an industrial LMD cell and calibrated. Some preliminary experiments, described below, have been carried out,

providing good results. To further validate the accuracy and repeatability in robot coordinates, a more comprehensive set of experiments is currently being conducted.

First, a manual scanning (arbitrarily moving the robot with a joystick) was performed, and the diameter of the holes on the working table (see Figs. 2 and 6) was computed through a best ellipse approximation. The real dimension is 16 mm and the calculated ones ranged from 16.05 to 17.09mm, yielding an average value close to 16.5mm, i.e., an average accuracy close to 0.5mm. It has to be noted that experiments can only be carried out in short inactive periods of time between fabrication runs. Thus, no particular setup can be applied to optimizing the performance of the proposed system, but the one used in the immediately previous fabrication run is also applied for the experiment.

After that, a real part was scanned on-line (Fig. 7). The results obtained can only be checked for the moment qualitatively, because point cloud processing (a subject of current work) is required for obtaining 3D measurements of parts. This issue is addressed in the aforementioned additional experiments being conducted.

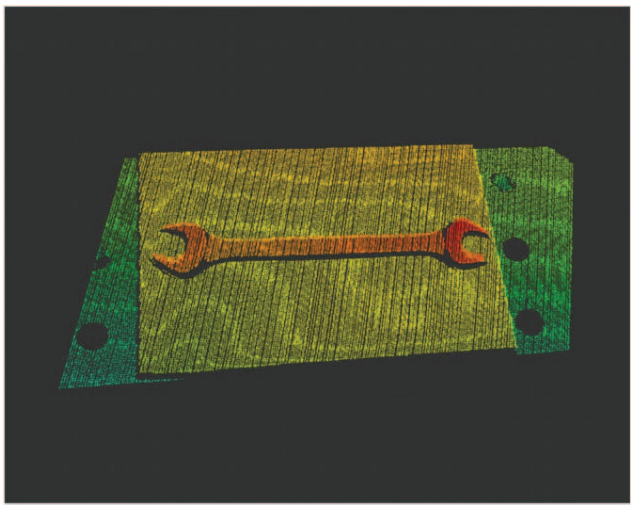

Fig. 7. 3D point cloud showing a real part scanned on-line.

During the last preliminary experiments, the system was tested with the LMD cell working in different cladding conditions. Multiple clad tracks have been deposited with different process speeds (8, 10 and 12 mm/s) and different laser power (from 1000 to 1400W). The base material and the powder material were both 1.2344 tool steel in all cases. Comparison of the computed measurements and the ones made on the actual fabricated parts confirm that the system achieves a dimensional accuracy close to 0.5mm independently of robot tool movement (i.e., speed, path, and orientation). Additional experiments will be conducted to more comprehensibly characterize the system.

VI. Conclusion

A 3D on-line scanning system for geometrical monitoring of industrial robotized LMD processes has been presented. It provides an efficient, cost effective, and flexible solution, capable of working with different cell configurations and operating conditions, thanks to the proposed self-calibration procedure. Moreover, the use of ROS-Industrial results in a robot-independent, standardized solution.

The monitoring system generates a 3D point cloud in robot coordinates without imposing constraints to the movement of the robot, achieving a resolution around 0.5mm. This implies a step forward in the state of the art, since to the best of authors' knowledge no current monitoring method exists capable of unconstrainedly working in robot coordinates with 6 degrees of freedom. Besides, the self-calibration procedure simplifies the otherwise tedious setup tasks.

Another significant feature from an industrial perspective is the ability of the system to work with large parts (in the range from cm to m).

All these characteristics, supported by preliminary experimental results, make the proposed approach particularly suitable to serve as basis for the development of an efficient on-line industrial LMD path control system with dynamic parameter adaptation capabilities. This will be the next step of this research.

Currently, additional experiments are being conducted to further characterize the system, which has just been installed in the fabrication cell.

References

[1] E.Toyserkani, A.Khajepour, and S.F.Corbin, *Laser cladding*, CRC press, 2004, pp. 1-18.

[2] L.Song and J.Mazumder, "Feedback control of melt pool temperature during laser cladding process", *IEEE Trans. Control Systems Technology*, vol. 19, no. 6, pp. 1349-1356, Nov. 2011.

[3] J.T.Hofman, B.Pathiraj, J.van Dijk, D.F.de Lange, and J.Meijer, "A camera based feedback control strategy for the laser cladding process", *Journal of Materials Processing Technology*, vol. 212, no. 11. pp. 2455-2462, Nov. 2012.

[4] J.Rodriguez-Araujo, J.J.Rodriguez-Andina, J.Farina, F.Vidal, J.L.Mato, M.A.Montealegre, "Industrial laser cladding systems: FPGA-based adaptive control", *IEEE Industrial Electronics Magazine*, vol. 6, no. 4, pp. 35-46, Dec. 2012.

[5] L.Song, V.Bagavath-Singh, B.Dutta, and J.Mazumder, "Control of melt pool temperature and deposition height during direct metal deposition process", *The International Journal of Advanced Manufacturing Technology*, vol. 58, no. 1-4, pp. 247-256, Jan. 2012.

[6] T.A.Davis and Y.C.Shin, "Vision-based clad height measurement", *Machine Vision and Applications*, vol. 22, pp. 129-136, 2011.

[7] OpenCV Library, online: http://opencv.willowgarage.com/

[8] C.H.Chen and A.C.Kak, "Modeling and calibration of a structured light scanner for 3-D robot vision", in *Proc. 1987 IEEE International Conference on Robotics and Automation*, vol. 4, pp. 807-815, 1987.

[9] E.W.Y.So, S.Michieletto, and E.Menegatti, "Calibration of a dual-laser triangulation system for assembly line completeness inspection", in *Proc. 2012 IEEE International Symposium on Robotic and Sensors Environments, ROSE 2012*, pp.138-143, 2012.

[10] M.A.Fischler and R.C.Bolles, "Random sample consensus: a paradigm for model fitting with applications to image analysis and automated cartography", *Communications of the ACM*, vol. 24, no 6, p. 381-395, Jun. 1981.

[11] R.Y.Tsai and R.K.Lenz, "A new technique for fully autonomous and efficient 3D robotics hand/eye calibration", *IEEE Trans. Robotics and Automation*, vol. 5, no. 3, pp. 345-358, Jun. 1989.